Aerodynamic Sensitivities of 2D High lift Airfoil Configured with Porous Trailing Edges

Pradeep Kumar* and Rolf Radespiel†

Technische Universität Braunschweig, 38108 Braunschweig, Germany

This study investigates the aerodynamic sensitivities of a two-dimensional (2D) high-lift airfoil equipped with porous trailing edges with the aim of noise reduction. The analysis is based on flow field data obtained from 2D Volume averaged Reynolds Averaged Navier-Stokes (VRANS) simulations of a high-lift airfoil with porous trailing edges and solid trailing edges. Experimental results for a reference case with solid trailing edge pursued in wind-tunnel are also presented. The results of simulations are compared for both types of trailing edges. The results show that the loss of lift coefficient due to the porous trailing edge is within the acceptable levels assuming the noise reduction is satisfactory.

I. Introduction

AIRCRAFT noise reduction is a major objective of the current collaborative research center SFB-880, located at the Technische Universität Braunshcweig, Germany. A significant portion of aircraft noise at approach conditions is due to flow noise of the high-lift system. The research center's concept for achieving very high-lift coefficients builds on circulation control using internally blown flaps.[1,2] The technology was greatly improved by combining the internally blown flap with a shape-adaptive leading edge[3] and by exploiting the synergies of blowing and boundary layer suction.[4] This high-lift concept alernates airframe noise by reducing aircraft speed during approach and take-off. Furthermore, the shape-adaptive leading edge removes the portion of slat noise from airframe noise. However, the trailing edge of the internally blown flap will now become a major source of airframe noise. It is known that porous trailing edges are an effective means for noise reduction in clean airfoils.[5,6] However, the implementation of the porous trailing edges is expected to alter the aerodynamic characteristics of the wings, possible resulting in reduced lift. It is important to predict these aerodynamic changes in order to minimize any unfavorable changes in the aerodynamic performance of the wing.

A set of extended Reynolds stress turbulence model equations for computing turbulent flows in porous media have been developed[7,8] previously within the research center. Initially, the validation of the numerical model was based on DNS-data of a generic channel flow[9] and later, wind-tunnel experiments for a 2D airfoil equipped with porous trailing edge were conducted[10,11] for further validation. This numerical model is used to study a number of test cases pf the present work where a porous trailing edge is implemented on a high lift airfoil with the aim to identify a porous material within 5% loss in lift while maintaining promising material properties for noise reduction. The porous material studied here closely resembles the properties of the material found to be effective in noise reduction.[5,6] Experimental validations for the high lift airfoil configuration are also underway, by conducting experiments at the low speed wind tunnel (MUB). The experiments for the reference wing without any porous inserts were recently concluded and are presented here for comparison with predictions from the numerical model.

Section II describes the numerical setup for the numerical simulations and the test cases considered in this study. Section III outlines the experimental setup for the reference airfoil used for validation of the numerical results. The numerical results are presented in section IV, followed by a comparison of aerodynamic coefficients between the airfoils with the porous and non-porous trailing edges. The final section, V, presents the conclusions and plans for the future work.

*Research Assistant, Institute of Fluid Mechanics, TU Braunschweig.

†Professor and Head of Institute, Institute of Fluid mechanics, TU Braunschweig.

II. Numerical Setup

II.A. Numerical Flow Model

An efficient volume and Reynolds Averaged Navier-Stokes (VRANS) flow model for resolving the flow inside and over the porous media has been well documented[8,12] within the research center. The momentum and turbulent transport equations are extended by the Darcy's law with Forchheimer correction[13] in order to include the contribution of porous medium. The Reynolds-stress turbulence model JHh-v2[14] has been used as baseline model, extended by volume averaging of the Navier-Stokes equations. Special jump models are applied for the porous and non-porous interface in order to accurately resolve the boundary layer. These jump models introduce several special parameters into the turbulence equations. In the present model, a total of six model parameters that govern porous medium - turbulence interactions are included, two of which account for the jump of velocity and turbulence stresses across the interface. A porous material is specified in the numerical model by providing porosity ϕ, permeability κ and Forchheimer coefficient C_F.

These equations have been implemented into the existing flow solver code DLR-TAU.[15] The model has been previously calibrated with DNS-simulations of Breugem[9] and with experiments[10] for a DLR-F16 airfoil.

II.B. Numerical Simulations

2D Volume and Reynolds averaged Navier-Stokes (VRANS) simulations of a flow around the DLR-F16 airfoil modified with a droopnose and a Coanda flap are performed. This modified airfoil has been specially designed as part of the current collaborative research center to achieve high-lift requirements.[3,16] Note that the modified droopnose DLR-F16 airfoil with Coanda flap is referred to as the droopnose airfoil throughout this paper.

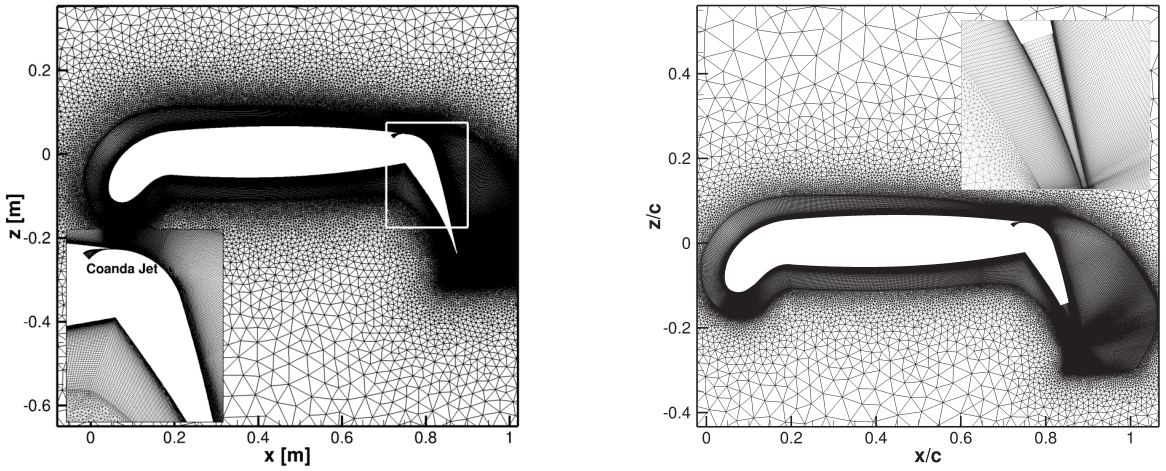

(a) (b)

Figure 1. Section of the numerical grid around (a) the droopnose airfoil with inset showing the location of the Coanda jet and (b) with porous trailing edge where the inset shows the grid inside the trailing edge for computations of the flow inside the porous medium.

The numerical grid for the droopnose airfoil, shown in Figure 1(a), consists of a structured mesh around the airfoil and an unstructured mesh everywhere else, which spans 50 chord lengths in all directions. The overall grid consists of around 265000 nodes. The structured mesh around the airfoil is constructed to resolve the boundary layer down to a dimensionless wall distance (y^+) value less than 1. The high resolution structured mesh is also extended to the flap area behind the airfoil as a greater computational accuracy is required in this region. The flap deflection angle is 65° and the airfoil chord-length is normalized to $1m$. Note that grid convergence studies have previously revealed that residual numerical errors on lift coefficient were smaller than 1%.[3] Ten percent of the airfoil chord at the trailing edge was replaced by porous material and meshed accordingly as shown in Figure 1(b). This resulted in an increase of three percent in overall

mesh points.

II.C. Test Cases

The VRANS simulations for Reynolds stress turbulence model were carried out using the DLR-TAU flow solver extended for the porous media as described in section II.A. The free stream conditions were set to match typical landing conditions of a cruise-efficient STOL aircraft,[17] which correspond to Reynolds number $Re = 12 \cdot 10^6$ and Mach number $Ma = 0.15$. Transition is set at 8 % on the suction side and at 30 % on the pressure side of the airfoil for the turbulence model. Transition locations are also set at the top and bottom of the plenum walls for the blowing jet. An additional transition location is manually set at 55 % on the pressure side to trip the attached flow ahead of the deflected flap.

The momentum coefficient C_μ of the blowing jet was controlled using a pressure boundary condition at the base of the plenum that is designed for blowing the air over the Coanda flap. The blowing intensity of a compressible jet is usually characterized by the momentum coefficient C_μ, defined as

$$C_\mu = \frac{\int \rho V_{jet}^2 \mathrm{d}A}{\frac{1}{2}\rho_\infty V_\infty^2 S_{ref}}$$

where V_{jet} is the jet velocity across the blowing slot exit, A is the slot exit area, S_{ref} is the reference area, ρ is the flow density, and the subscript ∞ refers to the freestream conditions.

The mean flow field contours allow for a simple visualization of the flow over the airfoil. The mean flow field at Reynolds number $Re = 12 \cdot 10^6$ for the no blowing case is presented in Figure 2. As the figure shows, the flow behind the flap is fully separated over the entire flap. However, the Coanda effect comes into play with blowing and as a result the separation location moves with the blowing intensity. An optimal blowing momentum coefficient $C_\mu = 0.035$ has been suggested[3] for the Reynolds number $Re = 12 \cdot 10^6$. This value is selected such that the flow is just attached up to the trailing edge for a broad range of angles of attack. Close to the maximum lift however, a local flow separation occurs that is embedded between the external flow and the wall jet, see Figure 6(a) as an example.

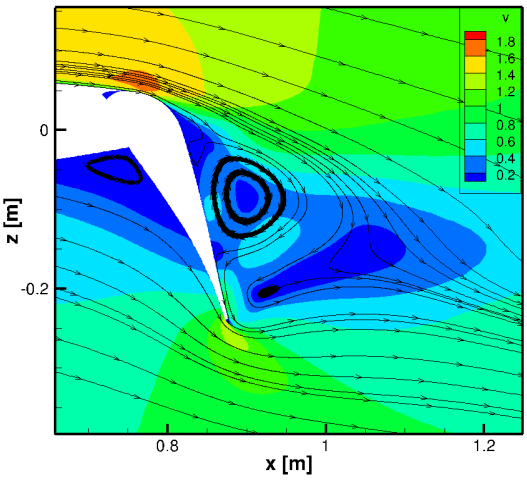

Figure 2. Mean flow field around the droopnose airfoil at $Re = 12 \cdot 10^6$ for the no blowing case.

In order to identify the dependence of C_{Lmax} on the porous materials, a hypothetical porous material based on the previously known materials[6,10] as listed in table 1 is studied numerically. The abbreviations in this table stand for PA: porous aluminum, SBP: sintered bronze powder and SFF: sintered fibre felts. It is important to note that the Forchheimer coefficient for these materials has not been measured and is approximated[10] to be $C_F = 0.1$ for all of these materials. The hypothetical material has porosity $\phi = 0.50$ and permeability $\kappa = 1.0 \times 10^{-10}$ within the limits of known materials in table 1. Furthermore, the jump coefficients briefly discussed in section II.A are still unknown for the materials presented in table 1 as they depend on the detailed material characteristics at the interface. Note that an effort to identify these parameters is underway. These jump coefficients have been set to *zero* for the purpose of this study.

III. Experimental Setup

The experiments for the reference condition without any porous insert inlay were recently concluded at the low speed wind tunnel Braunschweig (MUB) at Institute of Fluid Mechanics, TU Braunschweig. This is a Göttingen type facility with a closed test section with dimensions $1.3m$ x $1.3m$ where the turbulence level is about $T_u = 0.2\%$. The model based on the droopnose airfoil shown in Figure 1 is designed with a chord length of $0.3m$ to approximate 2-D flow at the midsection of the 1.3m long span and achieves a

Reynolds number $Re = 1 \cdot 10^6$ at 50 m/s in the wind tunnel. The midsection of the model is equipped with 63 static pressure tabs along the chord to obtain the pressure distributions. More pressure taps are clustered around the leading edge to capture the suction peak. During each pressure measurement, 100 samples were taken from the pressure tabs which were then averaged to get a mean pressure distribution. The data from pressure tabs was acquired using PSI systems.

The Coanda blowing at 70% chord is achieved with the help of a $3bar$ constant pressure compressor and the height of the jet exit slot is set to $0.0002m$. The blowing momentum C_μ is calculated[18] based on the pressure at the jet exit and plenum pressure, together with the mass flow rate entering the plenum measured using a FESTO 6444 flowmeter. Based on oil flow visualizations, it was found that the C_μ required for the attached flow at the flap is around $C_\mu = 0.062$ at the windtunnel Reynolds number.

Table 1. The properties of reference porous materials.[10]

Material name	porosity ϕ	permeability $\kappa[m^2]$
PA 80-110	0.46	1.24×10^{-10}
SBP 60	0.37	6.52×10^{-11}
SBP 120	0.36	2.80×10^{-10}
SFF 50	0.86	2.28×10^{-10}
SFF 120	0.89	1.91×10^{-10}

For the reference simulations using the numerical model discussed previously were also conducted for these experimental conditions at Reynolds numbers $Re = 1 \cdot 10^6$ to validate the results following the procedure explained in section II.C

IV. Results and Discussion

The numerical results are compared with the experimental data for the droopnose airfoil at $Re = 1 \cdot 10^6$. The effect of the porous trailing edges on the pressure distributions and on the maximum lift coefficients is presented later in this section.

IV.A. Comparison of numerical simulations with experiments

2D RANS simulations using RSM model were carried out to validate the experimental results. Transition tripping for the numerical model was set at 0.0036m on the suction side according to the observations made during experiments. It was also noted in the experiments that a transition location for the pressure side of the airfoil was difficult to realize due to the start of laminar bubble around the stagnation point. Two representative data sets at angle of attack $\alpha = 12^o$ and with blowing momentum coefficients $C_\mu = 0.05$ & $C_\mu = 0.062$ from the experiments are discussed here. The pressure distributions obtained from experiments are shown in Figure 3 with those obtained from the RSM model. The location of the blowing slot is seen as a vertical line in the pressure distributions in addition to two obvious suction peaks at about 8% and 80% on the suction side.

Table 2. Comparison of lift coefficients C_L at $\alpha = 12^o$

C_L for	$C_\mu = 0.050$	$C_\mu = 0.062$
Experiments	3.87	4.35
RANS	3.37	3.48

The numerical results follow the trends seen experimentally, however the amplitude of the suction peaks and overall pressure distribution C_p are much smaller in case of numerical simulations. The lift coefficients obtained from experiments and numerical simulations are shown in Table 2. The deviation in lift and pressure distribution is higher for the case of $C_\mu = 0.062$ than for $C_\mu = 0.050$, which could be due to the fact that the flow at the Coanda flap is attached for this condition in the experiments whereas for the numerical simulations the flow is already attached for $C_\mu = 0.050$. This can be seen from the mean flow fields for the two simulations shown in Figure 4. Since the flow is already attached at $C_\mu = 0.050$, a higher blowing of $C_\mu = 0.062$ does not greatly influence the lift as it does in experiments.

This significant disagreement between the numerical and experimental pressure distributions is likely due to a lack of the current Reynolds stress turbulence model to capture turbulent transport along the pressure side of the airfoil. We note the locally very low Reynolds numbers of the boundary layer on the pressure side. The Reynolds stress model yields very low Reynolds stresses along the entire lower airfoil surface, which resulted in very large recirculation regions at the droopnose and the flap hinge line. Further computations using Spalart Allmaras turbulence model[19] with curvature correction (SARC) are underway for scrutinizing the sensitivities with respect to the lower surface flow.

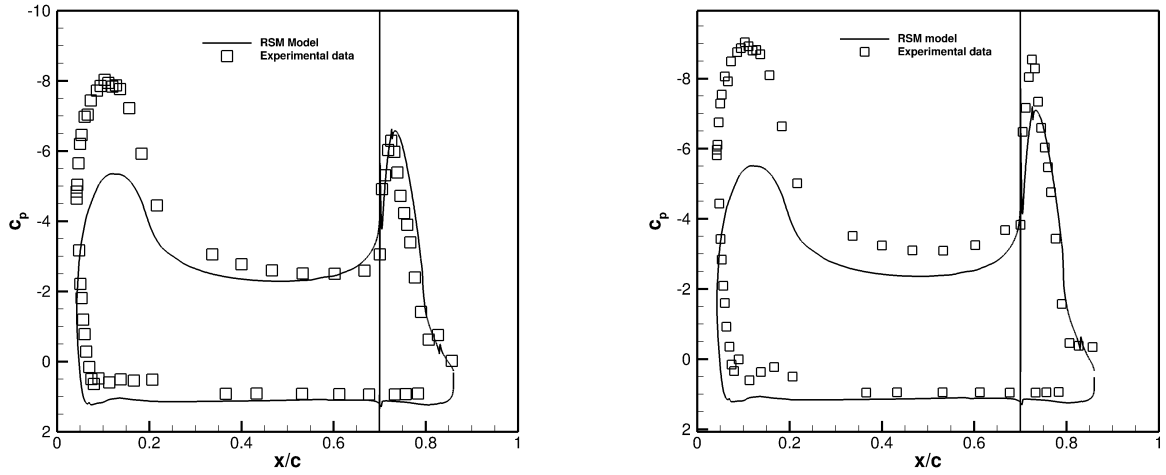

(a) (b)

Figure 3. Numerical and experimental pressure distributions over the droopnose airfoil at $\alpha = 12^o$ for (a) $C_\mu = 0.050$ and (b) $C_\mu = 0.062$.

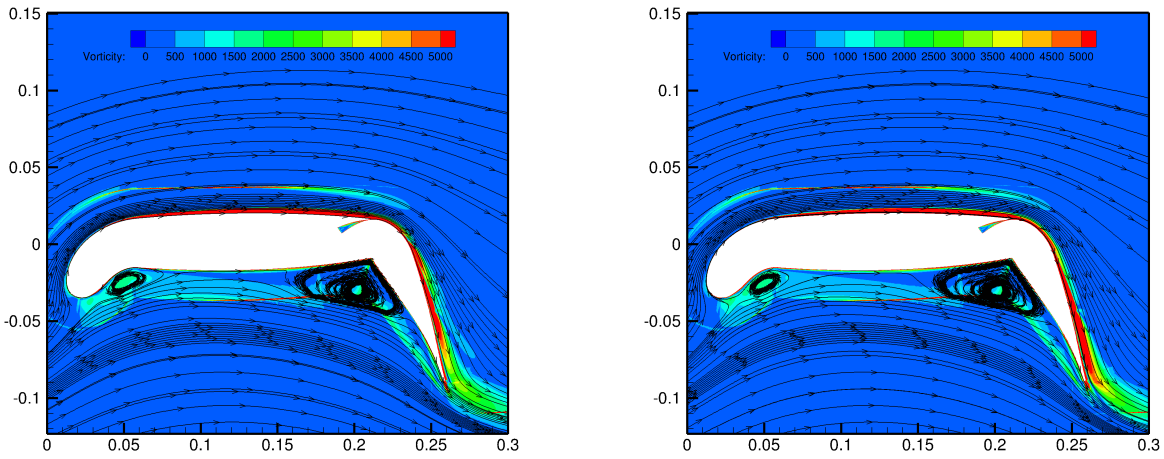

(a) (b)

Figure 4. Mean flow field around the droopnose airfoil at $\alpha = 12^o$ for (a) $C_\mu = 0.050$ and (b) $C_\mu = 0.062$.

IV.B. Reference configuration at $Re = 12 \cdot 10^6$

Numerical simulations at the desired Reynolds number $Re = 12 \cdot 10^6$ using SARC and RSM model were carried out to compare the results from the two models for the reference airfoil without any porous inserts. The previously obtained optimum $C_\mu = 0.035$ based on SARC simulations[3] is used for all configurations here. It is to be noted that for both models unsteady RANS simulations were required because of the presence of vortex shedding behind the flap as seen from Figure 2. The mean flow fields at the angle of attack, $\alpha = 12.25^o$ corresponding to the C_{Lmax} from the two models are shown in Figure 6. The flow at the flap is seen to be attached for the SARC simulations whereas for the RSM model, the flow is not attached all over the flap. It is possible that a slightly higher blowing C_μ is required for the RSM model to obtain attached flow for the whole flap. A smaller suction peak in the pressure distribution from the RSM model is observed when compared with that of the SARC model as seen in Figure 5. The lift coefficients are obtained $C_L = 5.0$ from the SARC model and $C_L = 4.58$ from the RSM model.

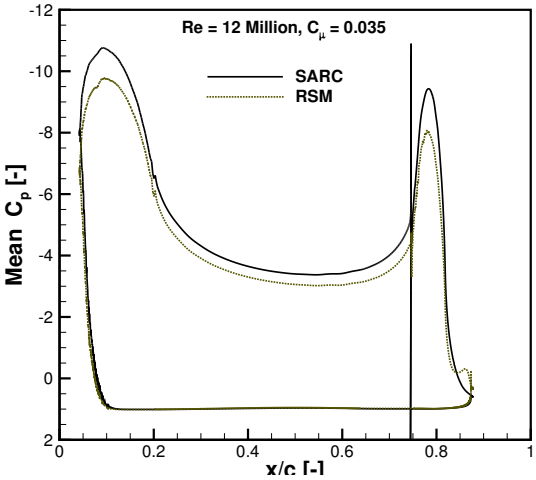

Figure 5. pressure distribution C_p at C_{Lmax} configurations for $Re = 12 \cdot 10^6$, $C_\mu = 0.035$ from the (a) SARC (b) RSM models.

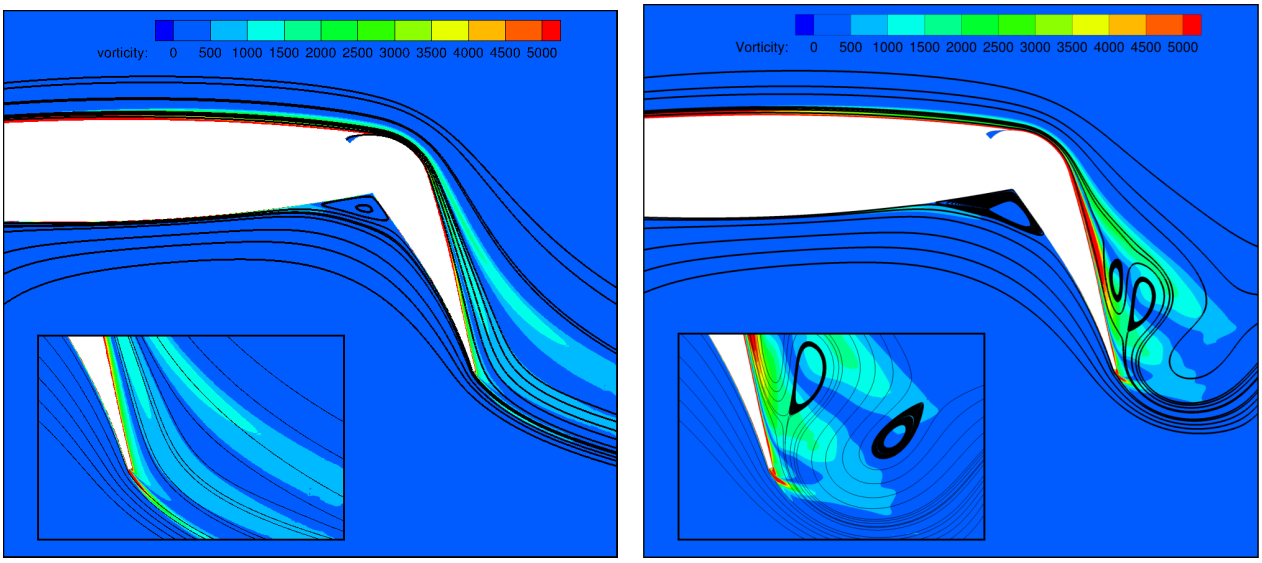

(a) (b)

Figure 6. Mean flow fields around the droopnose airfoil at C_{Lmax} configurations for $Re = 12 \cdot 10^6$, $C_\mu = 0.035$ from (a) the spalart allmaras with curvature correction (SARC) and (b) the Reynolds stress turbulence model (RSM).

IV.C. Effect of porous trailing edges on the pressure distributions

The results for the droopnose airfoil equipped with 10% porous trailing edge at a Reynolds number $Re = 12 \cdot 10^6$ from the simulations using RSM model are presented here. The material properties of the porous trailing edge are, porosity $\phi = 0.50$, permeability $\kappa = 1.0 \times 10^{-10}$ and Forchheimer coefficient $C_F = 0.1$. The comparison of pressure distributions for solid non-porous trailing edges with porous trailing edges at C_{Lmax} configuration i.e. $\alpha = 12.25^o$ and $C_\mu = 0.035$ is shown in Figure 7(a). The suction side pressure distributionC_p for the porous trailing edge lies below that for the solid trailing edge. This is an expected behavior[10] as the porous material lets the flow through the porous trailing edge which in turn leads to

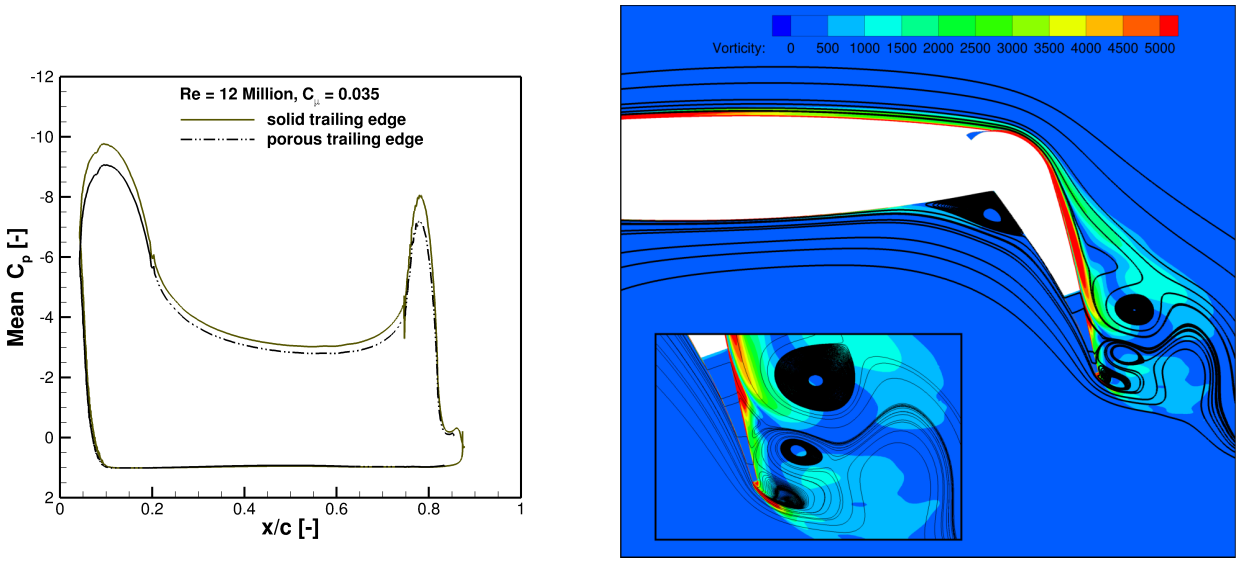

(a) (b)

Figure 7. (a) Pressure distributions for the solid and porous trailing edges and (b) mean flow fields around the droopnose airfoil at C_{Lmax} configuration for $Re = 12 \cdot 10^6$, $C_\mu = 0.035$.

smaller pressure differences over the suction side, as seen by examining the mean flow fields of the two types of trailing edges shown in Figures 6(b) and 7(b). The corresponding lift coefficient $C_L = 4.40$ for the droopnose airfoil with porous trailing edge is about 4% smaller than the $C_L = 4.58$ for the solid trailing edge airfoil. The passage of the flow through the trailing edge leads to significant changes of flow topology towards the trailing edge. Additional vortices with reverse flow are generated which contribute to increasing the wake width of Coanda flap, thus resulting in reduced lift generation.

A comparison of the lift curve obtained from uRANS simulations for the droopnose airfoil with porous and solid trailing edge is shown in Figure 8. It is seen that the lift is reduced at all angles of attack by approx. 4%.

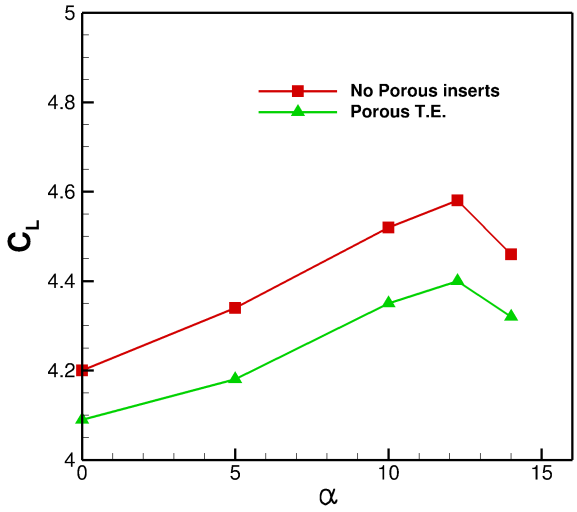

Figure 8. Mean flow field around the droopnose airfoil at $Re = 12 \cdot 10^6$ for the no blowing case.

V. Conclusions

The numerical results have been promising for Reynolds number $Re = 12 \cdot 10^6$ where the results address the possibility of finding a suitable porous material for high lift airfoil within acceptable losses in lift. The lift curves at an optimum blowing rate show that the loss of lift due to the porous trailing edges is relatively constant over a range of angles of attack. Experimental validations for the porous trailing edges are part of future measurement campaigns and should help understand the differences further.

The wind tunnel experiments for the reference airfoil configuration confirmed the general trends, however a good agreement is not achieved with numerical simulations. We believe that this behavior is a pitfall of the employed Reynolds stress turbulence model in representing transition to turbulent flow in complex boundary layers at low Reynolds numbers. This behavior needs to be further investigated. Computations with different turbulence models, for a range of blowing coefficients and angles of attack will be employed for this purpose.

Acknowledgments

This work is funded by the Deutsche Forschungsgemeinschaft (German research foundation) as part of the collaborative research center (SFB) 880 centered at the Technical University of Braunschweig.

References

[1]Radespiel, R., Pfingsten, K. C., and Jensch, C., "Flow Analysis of Augmented High-Lift Systems," *Notes on Numerical Fluid Mechanics and Multidisciplinary Design*, Vol. 102, Springer, Berlin, 2009.

[2]Pfingsten, K. C. and Radespiel, R., "Experimental and numerical investigations of a circulation control airfoil," *47th Aerospace Science Meeting*, AIAA, Orlando, 2009.

[3]Burnazzi, M. and Radespiel, R., "Design and Analysis of a Droopnose Configuration for Coanda Flap Applications," *Journal of Aircraft*, Vol. 51, No. 5, 2014.

[4]Burnazzi, M. and Radespiel, R., "Synergies between suction and blowing for active high-lift flaps," *CEAS Aeronautical Journal*, Vol. 6, No. 2, 2015, pp. 305–318.

[5]Herr, M. and Reichenberger, J., "In Search of Airworthy Trailing-Edge Noise Reduction Means." *AIAA-2011-2780*, 6 2011.

[6]Herr, M., Rossignol, K.-S., Delfs, J., Mößner, M., and Lippitz., N., "Specification of porous materials for low-noise trailing-edge applications." *20th AIAA/CEAS Aeroacoustics Conference, AIAA-2014-3041*, Atlanta, Georgia, 6 2014.

[7]Mößner, M. and Radespiel, R., "Numerical simulations of turbulent flow over porous media," *21st AIAA Computational Fluid Dynamics Conference, AIAA 2013-2963*, San Diego, California, 2013.

[8]Mößner, M. and Radespiel, R., "Modelling of turbulent flow over porous media using a volume averaging approach and a Reynolds stress model," *Computers & Fluids*, Vol. 25, No. 42, 2015.

[9]Breugem, W.-P., "The influence of wall permeability on laminar and turbulent flows," *Ph.D. thesis*, Technische Universiteit Delft, 2005.

[10]Mößner, M. and Radespiel, R., "Flow Simulations over Porous Media – Comparisons with Experiments," Eighth International Conference on Computational Fluid Dynamics ICCFD8-2014-0272, Chengdu, China, July 2014.

[11]Mößner, M. and Radespiel, R., "Flow simulations over porous media Comparisons with experiments," *Computers & Fluids*, 2017, pp. http://doi.org/10.1016/j.compfluid.2017.03.002.

[12]Mößner, M., "Volume-Averaged RANS-Simulation of Turbulent Flow over Porous Media," *Ph.D. thesis*, NFL Forschungsbericht 2016-01 ISBN 978-3-928628-79-2, 2016.

[13]Whitaker, S., "The Forchheimer equation: A theoretical development," *Transport in Porous Media*, Vol. 25, 1996, pp. 2761.

[14]Cecora, R.-D., Eisfeld, B., Probst, A., Crippa, S., and Radespiel, R., "Differential Reynolds stress modeling for aeronautics," *50th Aerospace Sciences Meeting*, AIAA 2012-0465, Nashville, Tennessee, 2012.

[15]Schwamborn, D., Gerhold, T., and Heinrich, R., "The DLR TAU-Code: Recent Applications in Research and Industry," *ECCOMAS CFD 06*, edited by P. Wesseling, E. Oate, and J. Priaux, TU Delft, The Netherlands, 9 2006.

[16]Burnazzi, M. and Radespiel, R., "Assessment of leading-edge devices for stall delay on an airfoil with active circulation control," *CEAS Aeronautical Journal*, Vol. 5, No. 4, 2014, pp. 359–385.

[17]Weiss, T. and Heinze, W., "Overall Design Assessment of CESTOL Aircraft," *SFB 880 - Fundamentals of High-Lift for Future Commercial Aircraft*, NFL Forschungsbericht 2015-04 ISBN 978-3-928628-67-9.

[18]M., Y. E. S., Beck, N., Semaan, R., and Radespiel, R., "Challenges in the quantification of the momemtum coefficient of circulation controlled wings in experiments," .

[19]Shur, M. L., Strelets, M. K., Travin, A. K., and Spalart, P. R., "Turbulence Modeling in Rotating and Curved Channels: Assessing the Spalart-Shur Correction," Tech. rep., 2000.